Original Research Article

Exploring the Benefits of Rice Husk Waste: Synthesis and Characterization of Biochar and Nanobiochar for Agricultural and Environmental Sustainability

ABSTRACT

Rice husk waste is a significant byproduct of rice production in developing countries, with a vast annual production. This waste material has been extensively used as an adsorbent for various substances due to its adsorption capabilities. Biochar, a carbon-rich material produced through pyrolysis of biomass, has gained attention for its diverse applications in agriculture and the environment. In this study, rice husk biochar and nanobiochar were synthesized and characterized to explore their potential benefits for agricultural and environmental sustainability. The biochar was prepared by pyrolysis of rice husk at 500°C in a low-oxygen environment, followed by grinding and sieving. Nanobiochar was obtained by ball milling the biochar particles. The physical and physicochemical properties of both biochar and nanobiochar were evaluated, including bulk density (0.41 and 0.59 Mg m^{-3}), particle density (0.49 and 0.54 Mg m^{-3}), water holding capacity (168.6 and 178.5%), pH (8.4 and 7.3), electrical conductivity (0.31 and 0.45 dS m^{-1}), cation exchange capacity (26.3 and 24.1cmol (p^{+}) kg^{-1}), volatile matter content (21.91 and 18.90%) and particle size distribution. Spectral analysis techniques such as DLS, FTIR, XRD, SEM and EDX were used to examine the size, zeta potential functional groups, crystallinity, porosity and elemental composition of the samples. The results showed that nanobiochar exhibited improved physical characteristics, such as higher porosity and water retention capacity, compared to biochar. The elemental composition and volatile matter content differed between the two materials. Nanobiochar also had significantly smaller particle size (11 nm) and a stable zeta potential. These findings suggest that rice husk nanobiochar has great potential for applications in soil fertility enhancement, adsorption of contaminants and waste management. The study contributes to the understanding of the properties and applications of rice husk waste-derived biochar and nanobiochar, promoting their utilization for sustainable agricultural and environmental practices.

Key words: Rice husk biochar, riche nanobiochar, pyrolysis, ball milling, environmental sustainability

INTRODUCTION

In developing countries, approximately 97% of the annual rice husk production amounts to around 80 million tonnes worldwide [1]. Rice husk has been extensively utilized as an adsorbent for the effective removal of a wide range of substances, including 10 different cations such as heavy metals, as well as 11 diverse types of dyes [2; 3; 4]. Biochar is a carbon-rich material that is formed through the thermal breakdown of lignocellulosic biomass, achieved either by subjecting it to high temperatures with limited oxygen or in the absence of oxygen altogether [5]. The production of biochar typically involves a process known as pyrolysis, where the feedstock is subjected to thermochemical decomposition. This decomposition occurs through heating the feedstock at temperatures ranging from 350-700°C, within a low oxygen environment (<1%) [6]. Biochars possess diverse physicochemical properties, including variations in pore size, surface area and functional groups. These properties are influenced by factors such as feedstock type, pyrolysis temperature, residence time, pressure and reactor type, which impact biochar yields, properties and applications [7]. The particle size of biochar can vary across a range of micrometers to centimeters, depending on the specific pyrolysis technology utilized [8]. The process of reducing the size of biochar particles to create nanoscale dimensions, referred to as nanobiochar [9; 10]. The most frequently employed technique for the preparation of nanobiochar is ball-milling [11]. The surface area of nanobiochar is greater when compared to that of bulk biochar [9; 11]. Reducing the size enhances the properties of biochar, making nanobiochar highly suitable for various agricultural and environmental applications. These include enhancing soil fertility, delivering nutrients, retaining nutrients, promoting soil microbial activity, adsorbing contaminants from water and soil, and sequestering carbon [12]. In light of the considerable research conducted in recent times regarding the production, characterization, and applications of nanobiochar, there is currently a valuable opportunity to compile a study that encompasses these recent advancements. The main objective of this work is to explore the potential benefits of rice husk waste by synthesizing and characterizing biochar and nanobiochar. The aim is to investigate their suitability for promoting agricultural and environmental sustainability, specifically focusing on their properties and applications in adsorption, soil fertility enhancement and waste management.

MATERIALS AND METHODS

Preparation of Rice husk biochar

To make use of the abundant rice husk resources in India, biochar production was carried out using a modified 200 L capacity cylindrical metal drum developed by Venkatesh et al. [13] and CRIDA. The rice husk was thermochemically converted into biochar with a yield of 40-45% through pyrolysis at a temperature of 500°C for one hour in a low-oxygen environment (<1% O_2). The biochar was dried through air drying and subsequent oven drying at 60°C until a constant weight was achieved. The dried biochar was then ground and sieved through a 2 mm sieve for the preparation of nanobiochar and further analysis. Electric stirring was employed to reduce the particle size of the raw rice husk biochar, resulting in enhanced surface-to-volume ratios and the emergence of new surface features, both of which are advantageous for adsorption processes.

Preparation of nanobiochar from rice husk biochar

The process of preparing nanobiochar from rice husk biochar involved the utilization of ball milling, a top-down method that employs mechanical forces to reduce particle size [14]. This environmentally friendly and cost-effective process has gained significant attention, offering potential for large-scale nanopowder production [15]. The methodology described by Wang et al. [16] and Zhang et al. [17] was adopted with minor modifications for the separation of biochar nanoparticles. Initially, 100 g of rice husk biochar was weighed and sieved through a 2 mm sieve, followed by grinding in a pestle and mortar to obtain a fine powder. The powder was further sifted using a 0.5 mm sieve and ground again to a fine powder. Subsequently,

another round of sieving through a 0.25 mm sieve was performed, and the resulting material was collected and finely ground using a pestle and mortar. Ultimately, 60 g of rice husk biochar was obtained from the initial 100 g. To modify the surface of the rice husk biochar, alkaline wash using sodium hexametaphosphate (SHMP) was carried out. 100 g of rice husk biochar with a sieve size of 0.25 mm was weighed into a 2 L beaker and mixed with 500 ml of distilled water. The reaction mixture was continuously stirred at 60 revolutions per minute for 10 to 20 minutes. Then, 5 g of sodium hexametaphosphate (SHMP) was added to the stirring mixture at a temperature of 50 °C and stirred for 60 to 90 minutes at 400 revolutions per minute. The resulting mixture was diluted with distilled water, stirred at room temperature for an additional 60 to 90 minutes, and allowed to settle. The settled mixture was removed from the beaker, cooled and washed with distilled water until it formed a clear suspension close to pH neutral. The suspension was centrifuged at 8000 rpm for 15 minutes, and the solid portion was collected. The solid component was dried in an oven at 60 °C for 18 to 24 hours and subsequently transformed into a fine powder using a pestle and mortar. The final yield of nanobiochar obtained from 100 g of rice husk biochar ranged from 90 to 95 g. The particle size reduction achieved through this process improves surface-to-volume ratios and alters the characteristics of the particle surfaces, making nanobiochar highly suitable for adsorption and the production of nanobiochar-based fertilizers.

Characterization of rice husk biochar (RB) and rice husk nanobiochar (RNB)

Physical properties

Using the Core technique, the bulk density of rice husk biochar and rice husk nanobiochar were determined [18]. Utilizing the water pycnometer method, the particle density of RB and RNB were calculated [19]. The saturated water holding capacity of RB and RNB were measured using the Keen Rackzowski box method [20].

Physico-chemical properties

After continuous shaking for an hour, the pH of the biochar in the water (pHw) and the electrical conductivity (EC) in the water were measured at a 1:10 (w/v) ratio [21]. Following the method used by Yuan *et al.* [22] with a little modification, the cation exchange capacity (CEC) of the biochar was assessed.

Ultimate and proximate analysis

Ultimate or elemental analysis of biochar samples were done by carbon analyzer (Elementar) at 950 ºC temperature [23]. In the case of proximate analysis, ash and volatile matter content were determined using the Mukherjee *et al.* [24] method.

Spectral analysis

The size and zeta potential of the nanoparticles were assessed using Dynamic Light Scattering (DLS) in a compact scattering spectrometer after filtering the aqueous particles suspension through a 0.22 µm syringe-driven filter, providing information on hydrodynamic size and stability at low negative zeta potentials.

FTIR (Fourier Transform Infrared) spectroscopy measures the absorption of infrared radiation by a sample, providing information about the sample's functional groups and compounds. A range of 400-4000 cm^{-1} was scanned in transmittance mode after creating a homogeneous and transparent film by combining a small portion of the sample with KBr (1:200) crystal and pressing it (Tensor 27, BRUKER).

XRD analysis (Ultima IV, Rigaku, Japan) was performed to determine sample crystallinity, identify particle phases and locate Bragg's reflections. Using a Rigaku diffractometer with CuK radiation at 40 kV and 20 mA, scanning at a rate of 10° per minute, and comparing the observed XRD pattern with literature references to determine phase peaks.

To characterize the morphology, physical properties, spectral composition and chemical composition of the samples, SEM (S4800, Hitachi, Japan) analysis with a 1-2 mm palladium and gold alloy coating (20 kV beam energy) was performed. EDX analysis provided

qualitative elemental composition information, including C, O, Si, Mg, Ca, S, K, Fe, Mn, Cu, and Zn, using the same 20 kV beam energy, along with gold or palladium-coated biochar samples mounted on Al stubs.

RESULTS AND DISCUSSION

Physical and physico-chemical properties of RB and RNB

The bulk density (BD) of RB (biochar) was measured at 0.41 Mg m^{-3}, while RNB (nanobiochar) had a slightly higher BD of 0.59 Mg m^{-3}. However, RNB exhibited a lower particle density (PD) of 0.54 Mg m^{-3} compared to RB's PD of 0.49 Mg m^{-3}. This indicates that RNB had a higher porosity (56.3%) compared to RB (48.6%), allowing for increased water retention capacity, with RNB reaching a maximum water holding capacity (MWHC) of 178.5% compared to RB's MWHC of 168.6%. These findings suggest that the nanobiochar (RNB) has improved physical characteristics for water retention, making it a promising material for agricultural applications (Table 1).

The pH of RB (rice husk biochar) was measured at 8.4, while RNB (rice husk nanobiochar) had a slightly lower pH of 7.3. RB had a lower electrical conductivity (EC) of 0.31 dS/m compared to RNB's EC of 0.45 dS/m. However, RB exhibited a higher cation exchange capacity (CEC) of 26.3 cmol (p^+) kg^{-1} compared to RNB's CEC of 24.1 cmol (p^+) kg^{-1}. These results indicate that both biochars possess alkaline pH values and low electrical conductivity, suggesting their potential to influence soil pH and nutrient availability in agricultural applications (Table 2).

Ultimate and proximate analysis of RB and RNB

The rice husk biochar (RB) exhibited a total carbon (TC) content of 45.80% and total hydrogen (TH) content of 4.71%. The remaining portion consisted of total oxygen (TO) at 49.49%. RB had a carbon-to-nitrogen (C/N) ratio of 62.96. On the other hand, the rice husk nanobiochar (RNB) had a higher TC content of 51.35% and lower TH content of 3.58%, resulting in a TO content of 45.07%. RNB had a slightly lower C/N ratio of 60.87 compared to RB. These results indicate that both RB and RNB are carbon-rich materials with varying composition, which can have implications for their stability, nutrient cycling, and carbon sequestration potential when applied in agricultural and environmental systems (Table 3).

The rice husk biochar (RB) had a volatile matter (VM) content of 21.91%, ash content of 32.58%, and fixed carbon (FC) content of 45.51%. The rice husk nanobiochar (RNB) had a slightly lower VM content of 18.90%, higher ash content of 34.71%, and similar FC content of 46.39%. These results indicate that both RB and RNB have significant amounts of fixed carbon, suggesting their potential as stable carbonaceous materials with reduced volatile matter. The higher ash content in RNB may be attributed to the preparation process, which could have introduced additional inorganic residues during the nanobiochar production (Table 4).

Particle size distribution

The particle size distribution analysis revealed that the rice husk nanobiochar (RNB) had significantly smaller particle sizes (d.nm: 11) (Fig 1c) compared to rice husk biochar (RB) (d.nm: 2087.7) (Fig 1a) indicating successful development of RNB. The reduction in particle size in RNB led to enhanced homogeneity of pore distribution, increased surface area, total pore volume and average pore width, which are advantageous for improved water retention capacity. These findings suggest that RNB has great potential for effective soil nutrient applications due to its smaller particle size and enhanced water retention properties [25].

Zeta potential (ZP) distribution

Zeta potential (ZP) is a crucial parameter that indicates the surface potential and charge of particles in suspension. It plays a significant role in determining various interactions and behaviours of particles, such as agglomeration, sedimentation and complexation with other substances. In this study, the ZP values of rice husk biochar (RB) (-47.6 mV) and rice husk nanobiochar (RNB) (-46.2 mV) were measured and depicted in Figure 1b and d, respectively. According to general stability criteria, particles with ZP values exceeding +30 mV or below -30 mV are considered stable [26; 27].

FTIR (Fourier Transform Infrared) spectroscopy

In this work, FTIR analysis was used to classify the samples into functional groups and identify the structural analysis modifications [28] between RB and RNB, the results are displayed in Figure 2a and b. When compared to rice husk biochar, RBN have more functional groups and several newly developing peaks. In comparison to rice husk biochar, most of the RNB sample showed the peaks of -COOH and C-H (2979 cm^{-1}, 2896 cm^{-1} and 1077 cm^{-1}) and RNB adsorption intensity was much higher than that of RB [29; 30]. For the majority of RNB, the peak of the O-H stretching vibration at 3866 cm^{-1} increased significantly [31]. Additionally, the C-O peaks for RNB, increased within the range of 1071-1384 cm^{-1}. Furthermore, as the particle size decreased, the conjugation effect weakened, shifting the aromatic -C=C or/and -C=O peaks to a higher wavenumber. For example, the peak of C-N increased from 1091 cm^{-1} for rice husk biochar to 1077 cm^{-1} for RNB, These findings indicated a reduction in conjugated benzene rings in RNB [29; 32]. Indicating the lowest aromaticity of RNB was the mild aromatic CH out-of-plane peaks in the fingerprint area (955 cm^{-1}, 953 cm^{-1}, 951 cm^{-1}, 797 cm^{-1}) and the strong intensity of C-H stretching of aliphatic CHx at 2979 cm^{-1}. These outcomes were consistent with the increased H/C index [29]. Plant sourced biochar with more -COOH and other C-O functional groups may be more readily to offer sorption sites for organic contaminants in environment. In comparison to rice husk biochar, RNB tended to have more functional groups and aliphatic chains, indicating their high reactivity in the environment. These functional groups provide valuable information about the chemical composition of the rice husk biochar and rice husk nanobiochar, which can have implications for its properties and potential applications such as soil amendment, water treatment and carbon sequestration. Further analysis and complementary techniques would help in a more comprehensive understanding of the biochar's composition and its various applications.

XRD (X-Ray Diffraction analysis)

One of biochars most distinguishing qualities was its mineral content, which gave rise to a number of uses [30]. XRD was used to characterise the mineral makeup of RB and RNB **(**Fig. 3a and b). The diffuse graphite peaks in the low and high theta regions, respectively, correspond to three groups of diffraction patterns that were typically recorded over the studied 2θ range ($0\text{-}80^0$) in the majority of cases. The presence of short-range order in the carbon structure is typically characterised by diffuse and broad bands in XRD patterns, whereas highly crystalline phases with a high degree of long-range order are confirmed by sharp and narrow peaks. This is due to the loading of the graphitic basal planes in carbon materials with long-term structural order and is typically seen at a 2θ value of 25^0 [33]. The XRD analysis was used to determine how different biochar samples formed crystalline or amorphous silica. All samples (RB and RNB) crystallinity peaks were found between 20° and 33° (at 2θ), which indicates that there is a significant reduction in the amount of amorphous solids present, the removal of organic components, and appropriate material stability. The existence of quartz (SiO_2) and calcite ($CaCO_3$), respectively, can be inferred from the presence of two distinct, strong crystalline peaks at 2θ at 26.62^0 and 30.14^0 and shows that there is cellulose present, which gives crystallinity to the particles. Peaks at $2\theta = 20^0\text{-}30^0$ denote the aromatic layers stacking arrangement (graphite). Sharp, unlabeled peaks in the

biochar suggest various inorganic constituents. All samples have a better crystalline structure, according to the XRD data, which was confirmed and it is a result of SiO_2 being present in the rice husk biochar. This is a high-energy site that is employed for adsorption in a preferred manner [34]. The heterogeneous nature of the rice husk biochar surface was confirmed by the X-ray diffraction peak. In addition to quartz (SiO_2) and calcite ($CaCO_3$), the samples also contain certain related minerals, including cristobalite (SiO_2), potassium oxide (KO_2) and moganite (SiO_2),

Scanning electron microscopy (SEM)/energy dispersive X-ray spectroscopy (EDX)

SEM images at different resolutions (500 µm, 100 µm, 20 µm, and 10 µm) were used to characterize the physical and morphological properties of rice husk biochar and rice husk nanobiochar (Fig. 4 a-h). [35; 36]. The images revealed irregularly shaped particles with a rough and porous surface for both biochar samples. The higher resolutions allowed for the observation of finer details, such as cracks, gaps and a network of interconnected pores. Rice husk nanobiochar exhibited additional nanoscale features, suggesting structural modifications due to the synthesis process. The porous structures and varying pore sizes indicate potential applications in adsorption and catalytic processes. Further analysis can explore the chemical composition and specific pore properties of these materials.

EDX surface elemental analysis (C, O, N, Fe, Na, Si, P, Cl, K, and Fe) was performed in concurrently with SEM. The analysis focused on different regions, as depicted in Figures 5 a-b and presented in the table 5, to identify and quantify the elemental composition of the samples.

The SEM-EDX analysis reveals that rice husk biochar (RB) consists of 19.10% carbon, 37.85% oxygen, 27.68% silicon, 0.69% nitrogen, and 4.16% potassium. In contrast, rice husk nanobiochar (RNB) contains 33.03% carbon, 35.01% oxygen, 24.33% silicon, 0.17% nitrogen, and 1.17% potassium. RNB exhibits lower silicon, potassium and nitrogen content compared to RB, possibly due to the nanobiochar production process. These results provide insights into the elemental composition differences between the two samples and their potential applications.

SUMMARY AND CONCLUSION

In this study, rice husk biochar (RB) and rice husk nanobiochar (RNB) were compared for their physical and physicochemical properties. RNB exhibited superior physical characteristics, including higher porosity, water retention capacity, and smaller particle size compared to RB. These properties make RNB a promising material for applications in agriculture, such as soil amendment and water management. RNB also showed enhanced reactivity and potential for sorption of organic contaminants. The findings contribute to promoting sustainable practices in agriculture and environmental management. Further research is recommended to explore specific applications and evaluate the environmental impact of RB and RNB.

REFERENCES

1. Wong KK, Lee CK, Low KS, Haron MJ. Removal of Cu and Pb by tartaric acid modified rice husk from aqueous solutions. Chemosphere, 2007;50:23–28.
2. Ye H, Zhu Q, Du D. Adsorptive removal of Cd (II) from aqueous solution using natural and modified rice husk. Biores. Technol. 2010;101:5175-5179.
3. Akhtar M, Bhanger MI, Iqbal S, Hasany SM. Sorption potential of rice husk for the removal of 2,4-dichlorophenol from aqueous solutions: Kinetic and thermodynamic investigations. J. Hazard. Mater. 2006;128:44-52.
4. Abdel Salam OE, Reiad NA, El Shafei MM. A study of the removal characteristics of heavy metals from wastewater by low-cost adsorbents. J.Adv. Res. 2011;2:297-303.

5. Al-Wabel MI, Hussain Q, Usman AR, Ahmad M, Abduljabbar A, Sallam AS. Impact of biochar properties on soil conditions and agricultural sustainability: a review. Land Degrad. Dev. 2018;29:2124-2161.
6. Oleszczuk P, Cwikła-Bundyra W, Bogusz A, Skwarek E, Ok YS, Characterization of nanoparticles of biochars from different biomass. J. Anal. Appl. Pyrolysis. 2016; 121:165–172.
7. Mohan D, Sarswat A, Ok YS, Pittman Jr CU. Organic and inorganic contaminants removal from water with biochar, a renewable, low cost and sustainable adsorbent-a critical review. Bioresour. Technol. 2014;160:191-202.
8. J. Lehmann, S. Joseph, in: J. Lehmann, S. Joseph (Eds.), Biochar for Environmental Management: Science, Technology and Implementation, seconded. Routledge, 2015.
9. Shan D, Deng S, Zhao, Wang B, Wang Y, Huang J. Preparation of ultrafine magnetic biochar and activated carbon for pharmaceutical adsorption and subsequent degradation by ball milling. J. Hazard. Mater. 2016;305:156-163.
10. Naghdi M, Taheran M, Brar SK, Kermanshahi-Pour A, Verma M, Surampalli RY, Immobilized laccase on oxygen functionalized nanobiochars through mineral acids treatment for removal of carbamazepine. Sci. Total Environ. 2017a;584585:393-401.
11. Naghdi M, Taheran M, Brar SK, Rouissi T, Verma M, Surampalli RY. A green method for production of nanobiochar by ball milling-optimization and characterization. J. Cleaner Prod. 2017b;164:1394-1405.
12. Song B, Chen M, Zhao L, Qiu H, Cao X. Physicochemical property and colloidal stability of micron-and nano-particle biochar derived from a variety of feedstock sources. Sci. Total Environ. 2019;661:685-695.
13. Venkatesh G, Gopinath KA, Reddy KS, Reddy BS, Prasad JV, Rao GR, Pratibha G, G, Srinivasarao C, Chari GR, Prabhaka M, Kumari VV, Biochar production and its uses in rainfed agriculture: experience from CRIDA-NICRA. Res. Bull. 2018.
14. Deguchi S, Mukai SA, Tsudome M, Horikoshi K. Facile generation of fullerene nanoparticles by hand-grinding. Advanced Materials. 2006;18(6):729-732.
15. Charkhi A, Kazemian H, Kazemeini M. Optimized experimental design for natural clinoptilolite zeolite ball milling to produce nano powders. Powder Technology. 2010;203:389-396.
16. Wang D, Zhang W, Hao X, Zhou D. Transport of biochar particles in saturated granular media: effects of pyrolysis temperature and particle size. Environmental Science and Technology. 2013a;47 (2):821–828.
17. Zhang H, Luo Y, Makino T, Wu L, Nanzyo M. The heavy metal partition in sizefractions of the fine particles in agricultural soils contaminated by waste water and smelter dust. Journal of Hazardous Materials. 2013;248–249:303–312.
18. Veihmeyer FJ, Hendrickson AH. Soil density and root penetration. Soil Science. 1948;65:487-493.
19. Hernandez-Mena LE, Pecora AAB, Beraldo Al. Slow Pyrolysis of Bamboo Biomass: Analysis of Biochar Properties. Chemiical Engiineeriing Transactiions. 2014;37:115-120.
20. Keen BA, and Raczkowski H. The relation between the clay content and certain physical properties of a soil. Journal of Agricultural Sciences. 1921;11:441-449.
21. Lee Y, Park J, Ryu C, Gang KS, Yang W, Park YK, Jung J, Hyun S. Comparison of biochar properties from biomass residues produced by slow pyrolysis at 500°C. Bioresource Technology. 2013;148:196–201.
22. Yuan JH, Xu RK, Zhang H. The forms of alkalis in the biochar produced from crop residues at different temperatures. Bioresource Technology. 2011;102(3):3488−3497.

23. Nelson DW, Sommers LW. Total carbon, organic carbon, and organic matter. In: Page, A.L., R.H. Miller, and D.R. Keeney (eds.). Methods of soil Analysis. Chemical and Microbiological properties. Agronomy. 1982;9:301- 312.
24. Mukherjee A, Zimmerman AR, Harris W. Surface chemistry variations among a series of laboratory−produced biochars. Geoderma. 2011;163(3-4):247−255.
25. Duarte S, Glaser B, Cerri C. Effect of biochar particle size on physical, hydrological and chemical properties of loamy and sandy tropical soils. Agronomy. 2019;9:165. https://doi.org/10.3390/agronomy9040165.
26. Skoglund S. Difficulties and flaws in performing accurate determinations of zeta potentials of metal nanoparticles in complex solutions—four case studies. PLoS One. 2017;12. e0181735. https://doi.org/10.1371/journal.pone.0181735.
27. Lyklema J, Lyklema J, Particulate colloids. 1. Ed, Elsevier, Amsterdam. 2005.
28. Zhao J. Comparison of biochars derived from different types of feedstock and their potential for heavy metal removal in multiple-metal solutions. Sci. Rep. 2019;9:9869. https://doi.org/10.1038/s4159 8-019-46234-4.
29. Qu X, Fu H, Mao J, Ran Y, Zhang D, Zhu D. Chemical and structural properties of dissolved black carbon released from biochars. Carbon. 2016;96:759-767.
30. Zhao L, Cao X, Masek O, Zimmerman A. Heterogeneity of biochar properties as a function of feedstock sources and production temperatures. J. Hazard. Mater. 2013;1(9):256–257.
31. Keiluweit M, Nico PS, Johnson MG, Kleber M. Dynamic molecular structure of plant biomass-derived black carbon (biochar). Environ. Sci. Technol. 2010;44(4):1247-1253.
32. Fang Q, Chen B, Lin Y, Guan Y. Aromatic and hydrophobic surfaces of wood derived biochar enhance perchlorate adsorption via hydrogen bonding to oxygen containing organic groups. Environ. Sci. Technol. 2014;48(1):279–288.
33. Zhao B, Nartey OD. Characterization and Evaluation of Biochars Derived from Agricultural Waste Biomasses from Gansu, China. Proceedings of the World Congress on Advances in Civil, Environmental, and Materials Research, Busan, Republic of Korea. 2014.
34. Strnad S, Kreze T, Stana-Kleinschek K, Ribitsch V. Correlation between structure and adsorption characteristics of oriented polymers. Material Research Innovations. 2001;4(2-3):197-203.
35. Saeed AAH, Harun NY, Sufian S, Afolabi HK, Al-Qadami EHH, Roslan FAS, Rahim SA, Ghaleb AAS. Production and characterization of rice husk biochar and Kenaf biochar for value-added biochar replacement for potential materials adsorption. Ecological Engineering & Environmental Technology. 2021;22:1-8.
36. Chia CH, Gong B, Joseph SD, Marjo CE, Munroe P, Rich AM. Imaging of mineral−enriched biochar by FTIR, Raman and SEM–EDX. Vibrational Spectroscopy. 2012;62:248−257.

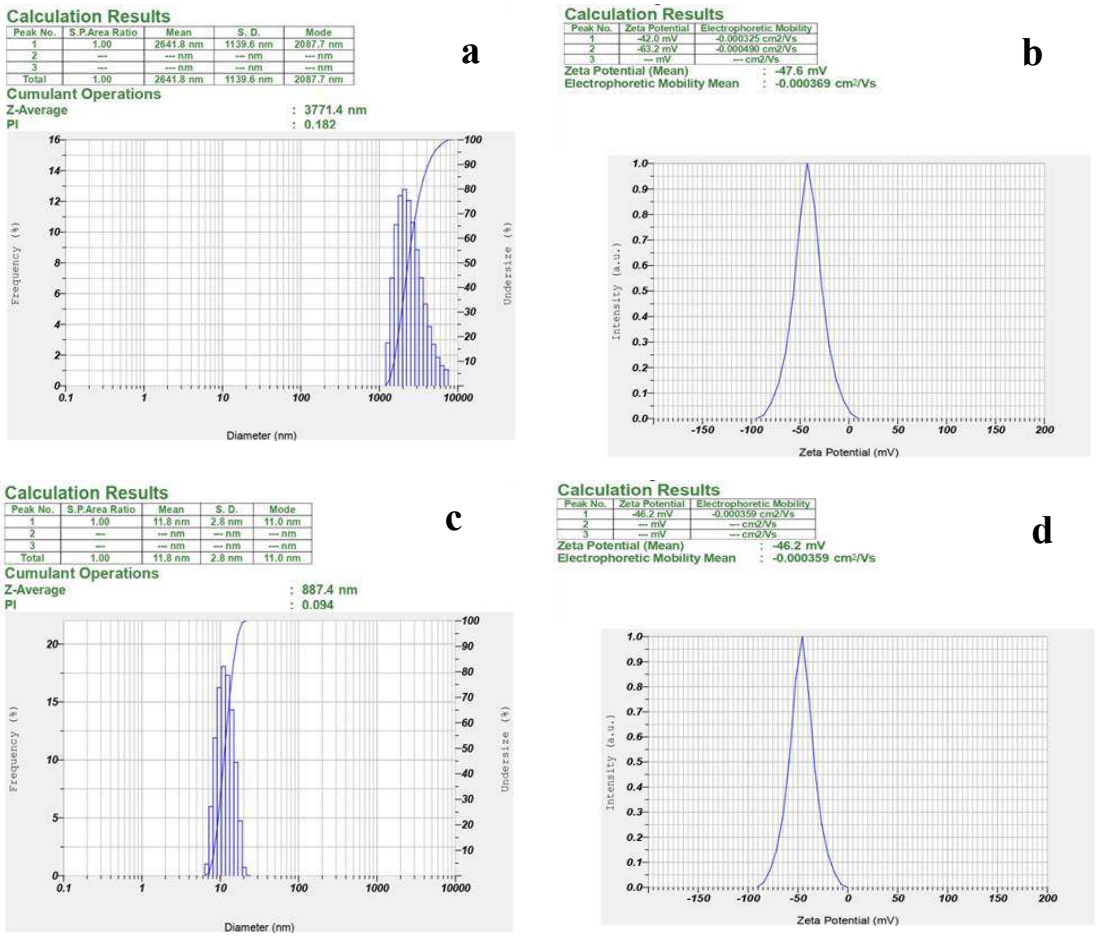

Fig.1. (a-d) Size and zeta potential of synthesized of (a) RB - (size: 2087.7 nm), (b) RB - (zeta potential: -47.6 mV) and (c) RNB (size: 11.0 nm), (d) RNB (zeta potential: -46.2 mV).

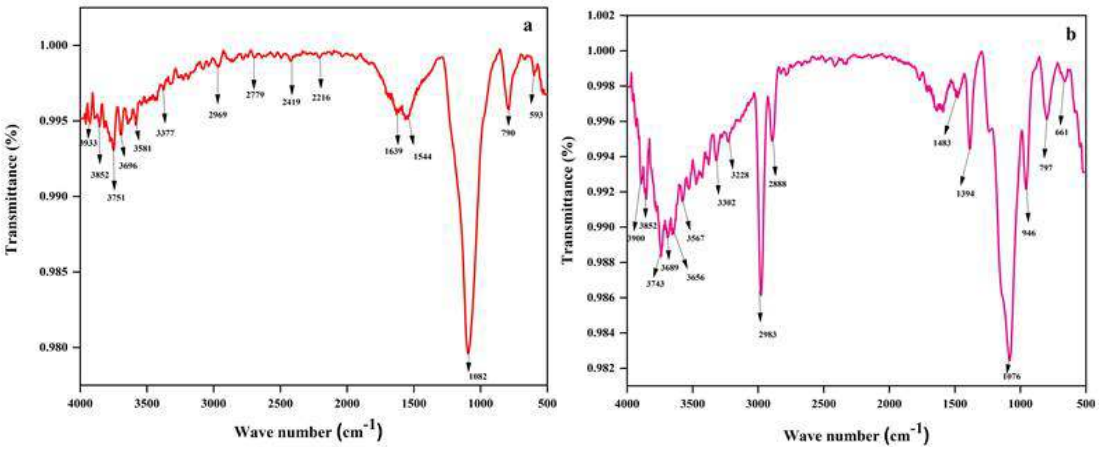

Fig. 2. (a-b) FT-IR micrograph provides evidence of distinct functional groups present on the surfaces of RB and RNB and more noticeable peaks size is observed in case of RNB (b) compare to RB (a).

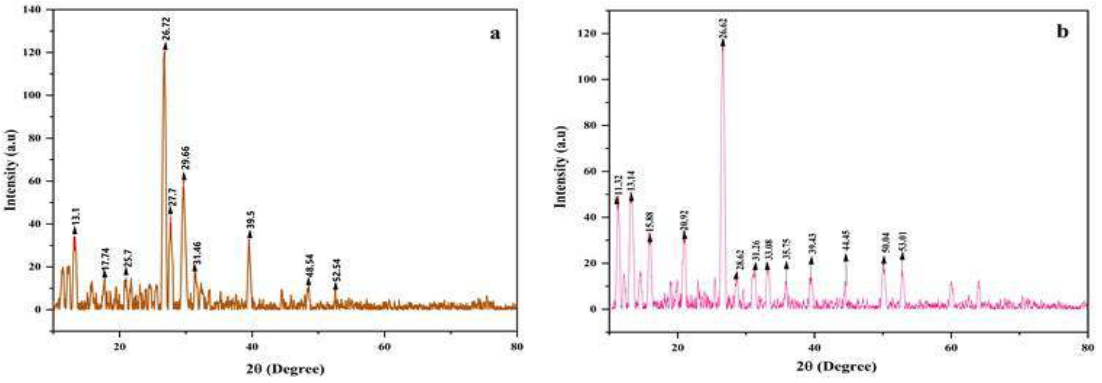

Fig. 3. (a-b) Crystal structure of the synthesized RB (Fig. 3a), RNB (Fig. 3b) were analyzed using XRD (X-ray diffraction). Distinctive diffraction peaks were observed in the crystal structure analysis of RB, specifically at 26.72, 27.7 and 29.66, while RNB exhibited n9otable peaks at 11.32, 13.14, 20.92 and 26.62.

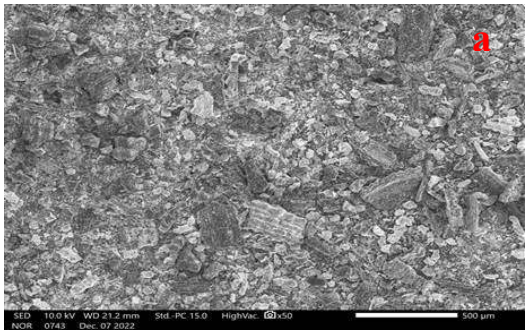
a
SED 10.0 kV WD 21.2 mm Std.-PC 15.0 HighVac x50 500 µm
NOR 0743 Dec. 07 2022

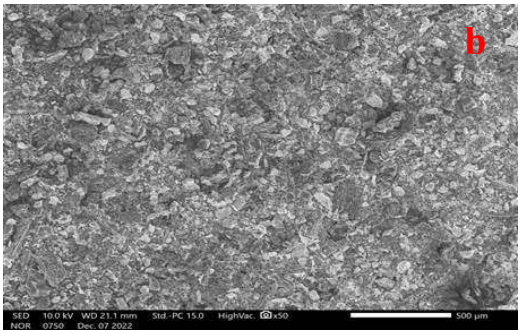
b
SED 10.0 kV WD 21.1 mm Std.-PC 15.0 HighVac x50 500 µm
NOR 0750 Dec. 07 2022

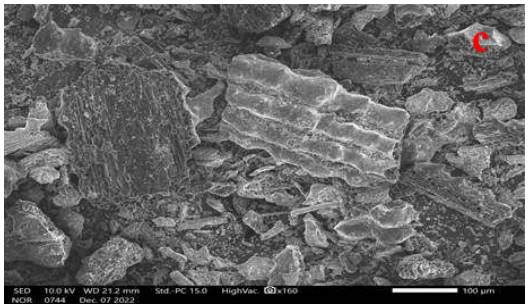
c
SED 10.0 kV WD 21.2 mm Std.-PC 15.0 HighVac x160 100 µm
NOR 0744 Dec. 07 2022

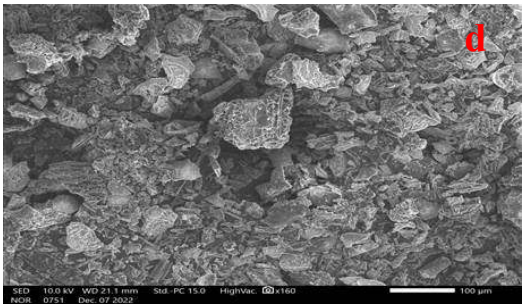
d
SED 10.0 kV WD 21.1 mm Std.-PC 15.0 HighVac x160 100 µm
NOR 0751 Dec. 07 2022

e f

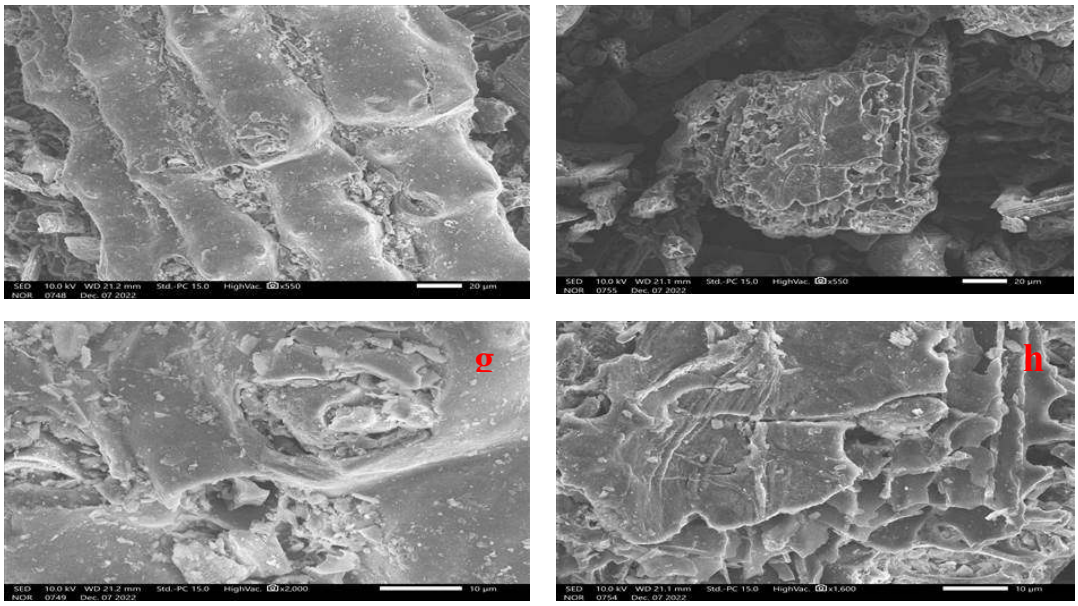

Fig. 4. SEM images of RB N and RNB at resolutions of 500 µm (a & b), 100 µm (c & d), 20 µm (e & f) and 10 µm (g & h), respectively, showing more porous structure of rice husk nanobiochar compare to rice husk biochar.

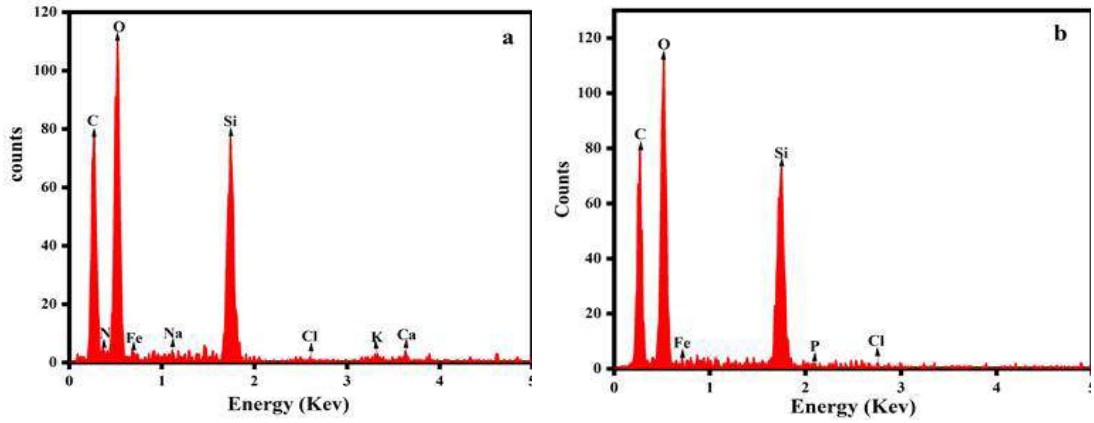

Fig. 5. Elemental analysis (EDX) of RB (a) and RNB (b) represents the detailed composition of nutrients.

Table 1. Physical properties.

Component	Bulk density (Mg m^{-3})	Particle density (Mg m^{-3})	Porosity (%)	Maximum water holding capacity (%)
RB	0.41	0.49	48.6	168.6
RNB	0.59	0.54	56.3	178.5

RB=Rice husk biochar, RNB=Riche husk nanobiochar

Table 2. Physico-chemical properties.

Component	pH (1:10)	EC (1:10)	CEC (cmol (p^+) kg^{-1})
RB	8.4	0.31	26.3
RNB	7.3	0.45	24.1

RB=Rice husk biochar, RNB=Riche husk nanobiochar

Table 3.Ultimate analysis of rich husk biochar and nanobiochar.

Component	TC (%)	TH (%)	TO (%)	C/N ratio
RB	45.80	4.71	49.49	62.96
RNB	51.35	3.58	45.07	60.87

RB=Rice husk biochar, RNB=Riche husk nanobiochar

Table 4. Proximate analysis.

Component	VM (%)	ASH (%)	FC (%)
RB	21.91	32.58	45.51
RNB	18.90	34.71	46.39

RHB=Rice husk biochar, RHNB=Riche husk nanobiochar

Table 5. Percentage of localized carbon, oxygen and some minerals content by SEM-EDX analysis of the samples (weight percentage).

Sample	Weight (%)				
	C	O	Si	N	K
RB	19.10	37.85	27.68	0.69	4.16
RNB	33.03	35.01	24.33	0.17	1.17